Chapter 3

Flow down an inclined plane

3.1 Introduction

Investigation of the properties of waves running down an inclined plane is a subject of great theoretical and practical importance and has attracted the attention of many researchers. Starting with the pioneering work of Kapitsa & Kapitsa [1], major contributions to this field have been performed in [2], [3], [4]. The physical picture is the following. A fixed flux of fluid is constantly poured on the inclined plane from above. The fluid forms a steady stream moving downwards under the action of gravity. A familiar example of such a flow is a river. Then, the influx of fluid upstream is suddenly increased. In a river, this may be caused by the melting of snow at regions neighbouring the river's source or by

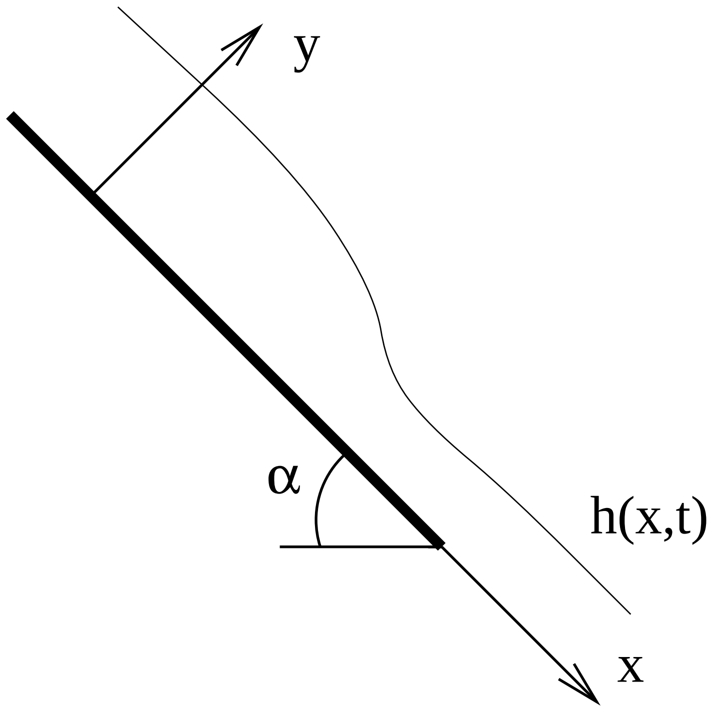

Figure 3.1: A wave running down an inclined plane.

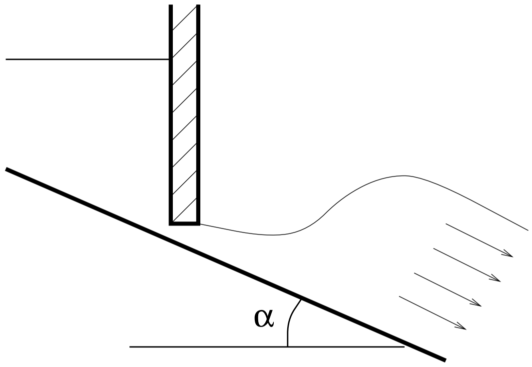

Figure 3.2: Stationary solutions correspond to the flow of water after a sluice.

rain. This causes the height upstream to increase, and the extra mass of fluid propagates downstream under the action of gravity. Under certain conditions, a solitary wave can be formed. In this case, the wave moves at a constant velocity c. In the system of coordinates moving together with the wave, the flow is stationary. Thus, all the variables depend on the combination $\xi = x - ct$, rather then on x and t separately, as illustrated in figure 3.1. We shall try to develop a theory for such waves, based on the method of averaging. We shall be interested in two questions. First, we would like to study when such solitary waves exist, and we shall study the solutions of the averaged equations depending on $\xi = x - ct$ (stationary solutions). Second, we would like to study whether such solitons are shocks. As we know from gas dynamics [5], the flow is supersonic in front of the shock wave and subsonic after the shock wave. In the moving coordinates with the shock wave, small disturbances in front of the wave can only propagate towards the shock (we shall call such a flow *supercritical* for the water waves). On the other hand, small disturbances after the shock can propagate both ways (we shall call such a flow *subcritical*). Thus, we shall perform a linear stability analysis of the averaged equations around two stationary states, before and after the shock.

In particular, setting $c = 0$ corresponds to stationary solutions. These stationary solutions describe, for example, the flow of water exiting from a sluice in the laboratory frame, as shown in figure 3.2. Such a flow is characterised by a region of rapid water flow immediately after the sluice, which then abruptly slows down and the layer of the water becomes thicker. We can also think of such a flow as a stationary hydraulic jump. Again, two questions will be of interest to us. First: when do such *stationary jumps* exist? Second: is it a shock, i.e., is the flow in front of it (in the shallow part) supercritical and the flow after the shock (in the deep part) subcritical? We shall show that our models provide physically reasonable solutions in this case also. We will only perform the linear stability analysis in the deep part of the flow, since the shallow part turns out to be of varying depth, and its stability analysis is quite complicated.

The speed c of the shock depends on how much the upstream level of water is increased, i.e., the height upstream h_2. Alternatively, we can consider c as a parameter, and study the existence of the solution $h \equiv const$ depending on c. This can be done using the exact Navier-Stokes equations, which is shown in the next section. We shall see that two solutions with $h \equiv h_1$ and $h \equiv h_2$ exist if c is sufficiently large. However, even if c is large enough and two stationary solutions exist, it is not at all clear that there exists a smooth solution connecting these two states. One can identify such a solution with a heteroclinic orbit, connecting two stationary states. To find out when such a heteroclinic connection is possible, we use integral methods.

We shall also note that the surface tension effects are neglected throughout the whole chapter. Only in the calculation of the linear stability shall we take these effects into account.

3.2 Necessary condition for the existence of a shock

Unlike the radial case studied in the previous chapter, the stationary solution for the full Navier-Stokes equations for this problem can be found analytically. We shall now derive this solution.

We assume that the fluid is viscous and incompressible. The full time-dependent Navier-Stokes equations for this problem are

$$\begin{aligned} &u_t + uu_x + wu_y = -\frac{p_x}{\rho} + \nu\Delta u + g\sin\alpha \\ &w_t + uw_x + ww_y = -\frac{p_y}{\rho} + \nu\Delta w - g\cos\alpha \\ &u_x + w_y = 0. \end{aligned} \tag{3.1}$$

The boundary conditions are

$$\begin{aligned} &h_t + q_x = 0 \\ &\sigma_{\tau n} = 0 \\ &\sigma_{nn} = p_0 \\ &u(y=0) = w(y=0) = 0. \end{aligned} \tag{3.2}$$

Here $h(x,t)$ is height, $u(x,y,t)$ is the x component of the velocity, $w(x,y,t)$ is the y component of the velocity, $p(x,y,t)$ is the pressure, $q(x,t) = \int u(x,y,t)\mathrm{d}y$, is the local flux, α is the inclination angle of the plane (see figure 3.1), σ is the stress tensor and $\Delta = \partial_x^2 + \partial_y^2$ is the Laplace operator. Equations (3.1.1-2) are the momentum equations. Equation (3.1.3) is the fluid's incompressibility. Equation (3.2.1) is the conservation of total mass flux. The dynamic conditions (3.2.2) and (3.2.3) are similar to (2.10) and (2.11), respectively. By (3.2.2), the force normal to the surface is balanced by the external pressure. Condition (3.2.3) requires that the force tangent to the surface vanishes. As usual, the subscripts t, x, y denote the partial derivatives with respect to t, x and y.

We shall make an assumption that the flow is of the solitary wave type. Thus, as we have mentioned, all the functions in (3.1-3.2) depend on combination $\xi = x - ct$ rather than two independent variables x and t. Hence, we have $\partial_x = \partial_\xi$, and $\partial_t = -c\partial_\xi$. The system (3.1) reduces to

$$\begin{aligned}
&-cu_\xi + uu_\xi + wu_y = -\frac{p_\xi}{\rho} + \nu\Delta u + g\sin\alpha \\
&-cw_\xi + uw_\xi + ww_y = -\frac{p_y}{\rho} + \nu\Delta w - g\cos\alpha \\
&u_\xi + w_y = 0,
\end{aligned} \tag{3.3}$$

where now $\Delta = \partial_\xi^2 + \partial_y^2$. The conservation of flux (3.2) becomes

$$-ch_\xi + q_\xi = 0, \tag{3.4}$$

which can be integrated to give:

$$-ch + q = Q = const. \tag{3.5}$$

One can see that the local flux

$$q(x,t) = \int u(x,y,t)\mathrm{d}y$$

is not a constant, but varies along the flow. In the laboratory system of coordinates, the flux upstream $q_2 = Q + ch_2$ is larger than the flux downstream $q_1 = Q + ch_1$ if $h_2 > h_1$.

The physical meaning of the constant Q in (3.5) is of the mass flux in the system of coordinates moving along with the solitary wave. In fact, if we go into the system of coordinates moving at the velocity c, the x component of the velocity of the fluid $u(x,y,t)$ in the new coordinate system has to be changed according to $u(x,y,t) \to u(x,y,t) - c$. Thus, the flux in the moving coordinate system will be

$$Q = \int_0^h \left(u(x,y,t) - c\right)\mathrm{d}y = q - ch, \tag{3.6}$$

and the conservation of Q gives (3.5).

Now we are ready to compute the stationary solutions of (3.3). Putting $\partial_\xi = 0$ everywhere in (3.3) gives identically $w = 0$ and $p = p_0 + \rho g\cos\alpha(h - y)$ from (3.3.2-3). Also, (3.3.1) reduces to

$$u_{yy} = -\frac{g}{\nu}\sin\alpha.$$

This equation can be easily integrated to give the parabolic profile for the velocity u:

$$u = -\frac{g\sin\alpha}{2\nu}\left(\frac{y}{h}\right)^2 + A\frac{y}{h} + B \tag{3.7}$$

From (3.4.4) we get $B = 0$ in (3.7). The shear-stress boundary condition in this case is just $u_y(y = h) = 0$. The velocity profile is thus

$$u = \frac{g\sin\alpha}{\nu}\left(\eta - \frac{\eta^2}{2}\right), \tag{3.8}$$

where $\eta = y/h$. The local flux is

$$q = \int_0^h u\mathrm{d}y = \frac{g\sin\alpha h^3}{3\nu}. \tag{3.9}$$

Given the flux downstream q_1, we can determine the stationary height downstream h_1:

$$h_1 = \left(\frac{3\nu q_1}{g\sin\alpha}\right)^{1/3} \tag{3.10}$$

The conservation of flux (3.5) requires that

$$\frac{g\sin\alpha h^3}{3\nu} - ch = Q = \frac{g\sin\alpha h_1^3}{3\nu} - ch_1. \tag{3.11}$$

The equation (3.11) always has at least one solution for the height $h = h_1$. The question is whether the second solution $h = h_2$ exists. Before we give an answer to this question, we shall transform the system (3.1) into a non-dimensional form, which will simplify the final expressions.

To bring the system (3.1) to a non-dimensional form, we choose the height of the stationary solution h_1 given by (3.10) as the length scale. Then, the velocity scale is given by $u_1 = q_1/h_1$, and the time scale is $h_1/u_1 = h_1^2/q_1$. The pressure is then rescaled by ρu_1^2. In the rescaled variables, (3.1) becomes:

$$\begin{aligned} u_t + uu_x + wu_y &= -p_x + \frac{1}{R}\Delta u + \frac{3}{R} \\ w_t + uw_x + ww_y &= -p_y + \frac{1}{R}\Delta w - \frac{3}{R}\cot\alpha \\ u_x + w_y &= 0, \end{aligned} \tag{3.12}$$

where the Reynolds number R is

$$R = \frac{u_1 h_1}{\nu} = \frac{q_1}{\nu}. \tag{3.13}$$

The conservation of flux (3.11) is just

$$h^3 - ch = 1 - c. \tag{3.14}$$

The parabolic velocity profile (3.8), characterising stationary solutions, is now

$$u = 3\left(\eta - \frac{\eta^2}{2}\right). \tag{3.15}$$

It is obvious that the solution with a parabolic profile and $h = 1$ is always a solution of (3.12-3.14). However, if c is large enough, other solutions with $h \neq 1$ are possible. The velocity profile of these solutions is parabolic (3.15), and the height is a solution of (3.14) with $h \neq 1$. In fact, we can rewrite (3.14) as

$$(h-1)(h^2 + h + 1 - c) = 0. \tag{3.16}$$

Solutions of (3.16) with $h \neq 1$ exist if $c > 1$. Thus, the height h_2 of such a non-trivial solution satisfies

$$h_2^2 + h_2 + 1 = c. \tag{3.17}$$

Thus, we can formulate the conclusion of this section:

1. If $c \leq 1$, only one stationary solution of (3.12)-(3.14) exists. The velocity has parabolic velocity profile, and height is $h \equiv 1$.
2. If $c > 1$, there are *two* stationary solutions with $h \equiv 1$ and $h \equiv h_2$ and a parabolic velocity profile. The height h_2 satisfies $1 + h_2 + h_2^2 = c$.

In the derivation of these solutions, no approximations were made. The solutions thus obtained are the exact solutions of the full Navier-Stokes equations.

The condition $c > 1$ for the existence of two stationary solutions is only the *necessary* condition for the existence of a solution going from $h = h_2$ at $x = -\infty$ to $h = h_1$ at $x = +\infty$. One cannot guarantee that such a solution will exist until the corresponding solution of (3.12) is found. The condition for the existence will be dependent on the relationship between the parameters in (3.12): R, α, c, and obtaining such a condition will be the ultimate goal of this chapter. However, if one uses the full system (3.12), obtaining the conditions for the existence of a solitary wave becomes a very difficult task. To simplify the problem, we shall derive the integral models of (3.12), which will allow us to find the relevant conditions for the existence of different types of solution.

In what follows, we shall make use of the relationship $c = 1 + h_2 + h_2^2$ (if $c > 1$) and use h_2 as a parameter, rather than c. This will considerably simplify the formulas. The condition $c > 1$ is now just $h_2 > 0$, and $h_2 > 1$ if $c > 3$. We shall now show that we only need to study the regime $h_2 > 1$ ($c > 3$), since there is a symmetry between the parameter regions $h_2 < 1$ and $h_2 > 1$.

3.3 Symmetry of the parameter domains $h_2 < 1$ and $h_2 > 1$

When two solutions $h = h_1$ and $h = h_2$ exist, our choice of h_1 as a length scale was arbitrary. In fact, we could as well have chosen h_2 to be the length scale. In this case, h_2 would have been 1 and we would use h_1 as the parameter. Thus, there is an intrinsic symmetry hidden in (3.12)-(3.14). In fact, let us suppose we additionally rescale the length scale by h_2: $h = \tilde{h}h_2$. In this case, $h_1 = 1$ becomes $\tilde{h_1} = 1/h_2$, and $\tilde{h_2} = 1$. We can interchange the indices 1 and 2, so we have $\tilde{h_1} = 1$ and $\tilde{h_2} = 1/h_2$. When we interchange the indices 1 and 2, we have to scale the Reynolds number, since we are using $R = q_2/\nu$ (in the old non-rescaled coordinates) instead of $R = q_1/\nu$. Thus, the Reynolds number scales as $\tilde{R} = Rh_2^3$ due to (3.13).

If we find a solution of (3.12)-(3.14) for the values of parameters h_2 (with $c = 1 + h_2 + h_2^2$), R and α, this solution will be connected through the rescaling $h = \tilde{h}h_2$ to the solution of (3.12) with the parameters $\tilde{h_2} = 1/h_2$ (with $\tilde{c} = 1 + 1/h_2 + 1/h_2^2$), $\tilde{R} = h_2^3 R$ and $\tilde{\alpha} = \alpha$. We can therefore draw the following conclusion:

A heteroclinic solution starting at $h = h_2$ at $x = -\infty$ and going into $h = 1$ at $x = +\infty$ for the parameters R, α exists if and only if a heteroclinic trajectory connecting the states $h = 1$ at $x = -\infty$ and $h = 1/h_2$ at $x = +\infty$ exists for the values of parameters Rh_2^3, α.

We shall use this symmetry to simplify the analysis of the solution in the parameter space h_2, R, α. Once the behaviour of the solutions in the part $h_2 > 1$ is determined, the results for $h_2 < 1$ can be decided using the symmetry.

Now, we shall commence derivation of the integral models for (3.12) and analyse the dependence of the resulting models with respect to the parameters h_2, R and α. The symmetry described above will help us to perform this analysis. We shall only be interested in the solutions of the type shown on figure 3.1, where the height upstream h_2 is larger than the height downstream, which is equal to 1 due to our rescaling.

3.4 Boundary layer approximation

As before, we shall assume that the layer of fluid is so thin that the boundary layer approximation can be applied to (3.12). Since the boundary layer approximation was described in sufficient detail in the previous chapters, we shall just write down the formulas without going into details its derivation. The reader not familiar with this approximation should consult chapters 1 and 2 of this thesis.

The system (3.12) in the boundary layer approximation simplifies to

$$\begin{aligned} &u_t + uu_x + wu_y = -\frac{3}{R}h_x \cot\alpha + \frac{1}{R}u_{yy} + \frac{3}{R} \\ &u_x + w_y = 0. \end{aligned} \tag{3.18}$$

The boundary conditions (3.2) become

$$\begin{aligned} &u(y=0) = w(y=0) = 0 \\ &u_y(y=h) = 0, \end{aligned} \tag{3.19}$$

and the conservation of mass is

$$h_t + \left(\int_0^h u\mathrm{d}y\right)_x = 0. \tag{3.20}$$

If we introduce the average velocity

$$v = \frac{1}{h}\int_0^h u\mathrm{d}y \tag{3.21}$$

the mass conservation (3.20) can be written as

$$h_t + (hv)_x = 0. \tag{3.22}$$

3.5 Averaging method for the boundary layer flows

In the derivation of the integral methods for the inclined plane we shall use the same procedure which was used to derive the integral models for the stationary hydraulic jump. First, we shall derive the integral equations for the self-similar profile, similar to (2.32). Then, we shall allow the profile to change by introducing an extra shape parameter Λ and get a system similar to (2.42).

3.5.1 Self-similar profile

We shall approximate the velocity profile as

$$u(x,y,t) = v(x,t) f\left(\frac{y}{h(x,t)}\right). \tag{3.23}$$

Here $v(x,t)$ is the average velocity given by (3.21), and $f(\eta)$ is a function satisfying

$$\begin{aligned} &f(0) = 0 \\ &f'(1) = 0 \\ &\textstyle\int_0^1 f(\eta)\mathrm{d}\eta = 1. \end{aligned} \tag{3.24}$$

For example, a parabola $f(\eta) = 3(\eta - \eta^2/2)$ satisfies (3.24). The unknown variables are $h(x,t)$ and $v(x,t)$. One equation is provided by (3.22). Another equation is the momentum equation (3.18), integrated from 0 to h:

$$\begin{aligned} &h_t + (vh)_x = 0 \\ &(hv)_t + (hv^2 F_2)_x + \tfrac{3}{R} h h_x \cot\alpha = -\tfrac{3}{R}\tfrac{v}{h} + \tfrac{3}{R}h, \end{aligned} \tag{3.25}$$

where $F_2 = \int_0^1 f^2(\eta)\mathrm{d}\eta$ is a constant for a given profile. In particular, $F_2 = 6/5$ for the parabolic profile. Equation (3.25) is the time-dependent, Cartesian analogue of (2.32).

To look for solitary waves propagating down with the speed c, we substitute $\xi = x - ct$ in (3.25). We get:

$$\begin{aligned} &-ch + vh = 1 - c \\ &-c(hv)_\xi + \tfrac{6}{5}(hv^2)_\xi + \tfrac{3}{R} h h_\xi \cot\alpha = -\tfrac{3}{R}\tfrac{v}{h} + \tfrac{3}{R}h. \end{aligned} \tag{3.26}$$

The system (3.26) can be rewritten as a first-order differential equation for h only:

$$h' = \frac{15}{R}\frac{(h-1)(h^2+h+1-c)}{(c^2h^2 - 6(1-c)^2 + 15h^3/(R\tan\alpha))}. \tag{3.27}$$

We shall now show that stationary shocks (shown in figure 3.2) cannot be described by (3.27).

Stationary shocks

If $c < 1$, equation (3.27) has only one fixed point $h = 1$. In this case, the physically relevant solution of (3.27) may describe, for example, the flow of water exiting a sluice, see figure 3.2, which corresponds to $c = 0$. For such a solution, the height vanishes at a finite ξ, and we shall now determine if such solutions are plausible in the model (3.27). We shall perform our analysis for an arbitrary c, even though the physically meaningful solutions (sluise-type solutions) correspond to $c = 0$. The case $0 \le c < 1$ is incorporated without an extra effort.

If h is very small, (3.27) simplifies to

$$h' = \frac{5}{2R(1-c)}. \tag{3.28}$$

We can see that only the case $c < 1$ can give physically meaningful solutions, since h' must be positive at the point where h vanishes. At the singular point ξ_0, corresponding to $h = 0$, the height grows as

$$h(\xi) = \frac{5}{2R(1-c)}(\xi - \xi_0). \tag{3.29}$$

We shall now investigate whether the solutions with the height vanishing at a certain ξ and smoothly connected to the fixed point $h = 1$, are possible for (3.27). The problem arises if the system (3.27) becomes singular between $h = 0$ and $h = 1$.

The denominator of the right-hand side of (3.27) vanishes and the derivative $h'(\xi)$ becomes infinite if h satisfies

$$f_d(h) = \frac{15h^3}{R\tan\alpha} + c^2h^2 - 6(1-c)^2 = 0. \tag{3.30}$$

Equation (3.30) has only one real solution h_*, and this solution is always positive for the physical values of the parameters R, α, c. The behaviour of (3.27) is qualitatively different depending whether $h_* < 1$ or not. If the value of the parameter $R\tan\alpha$ is made larger, the function $f_d(h)$, specified by (3.30), will grow more slowly with respect to h. Thus, the solution h_* of the equation $f_d(h) = 0$ increases when $R\tan\alpha$ is increased. Consequently, the condition for $h_* > 1$ is

$$R\tan\alpha > \frac{15}{6(1-c)^2 - c^2}. \tag{3.31}$$

There are two possible cases to consider. First, if $c < (6-\sqrt{6})/5 \simeq 0.7101$ (in particular, $c = 0$), the right-hand side of (3.31) is positive. Thus, the solutions smoothly connecting to $h = 1$, and with $h \to 0$ at finite ξ can only be realized if $R\tan\alpha$ satisfies (3.31). Second, if $(6-\sqrt{6})/5 < c < 1$, the right-hand side of (3.31) is negative. In this case, the singular height h_* is always larger than 1 and there is no restriction on $R\tan\alpha$. (We would like to emphasise once again that due to (3.29) such solutions are possible only for $c < 1$).

However, even if (3.31) is satisfied, the solution does not look like a stationary shock at all, as we illustrate on figure 3.3. There is no flat shallow part in the solution, and the height profile increases immediately to $h = 1$. We shall thus claim that such solutions are not the stationary shocks we are interested in.

We see that the self-similar profile is inadequate for describing stationary shocks. We shall now study whether the self-similar profile can predict moving solitary waves.

Solitary waves: $c > 1$

If $c > 1$, the system (3.27) has two fixed points: $h = h_1 = 1$ and $h = h_2$, where h_2 satisfies $h_2^2 + h_2 + 1 = c$. Since (3.27) is a first-order autonomous differential equation, the necessary condition for the existence of a heteroclinic orbit (a solution starting at h_1 and ending at h_2 or vice versa) is that one of the fixed points is stable and the other is unstable. For convenience, we substitute $c = 1 + h_2 + h_2^2$ in (3.27) and use $h_2 > 0$ as a parameter. Physically, it corresponds to changing the height upstream and then observing

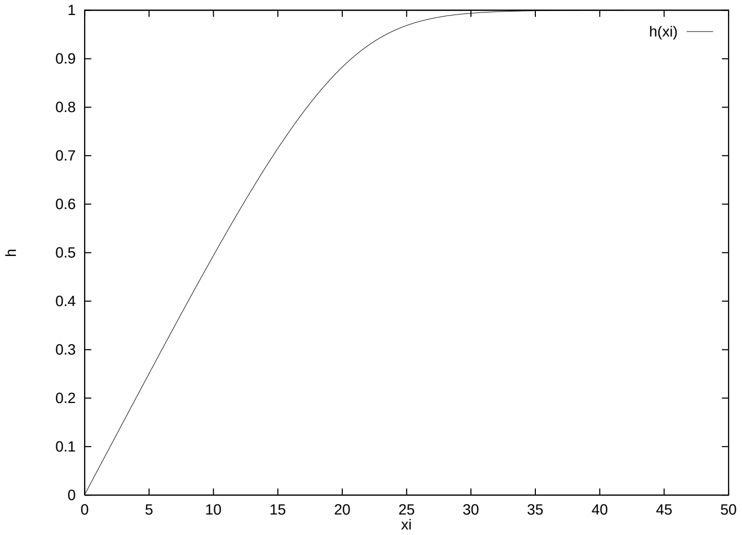

Figure 3.3: A solution of (3.27) for $R = 5, \alpha = 5$ deg and $c = 0$ corresponding to $h_* > 1$.

the corresponding change in the wave velocity. Due to the symmetry described before, we only have to study the case $h_2 > 1$. The point $h = 1$ is stable if

$$R \tan\alpha < \frac{15}{5h_2^4 + 10h_2^3 + 3h_2^2 - 2h_2 - 1} = f_1(h_2). \tag{3.32}$$

To study the stability of the fixed point $h = h_2$ in the sense of (3.27), we can use the symmetry considerations above. We rescale height $h \to h/h_2$. Under this rescaling $h_1 = 1$ becomes $\tilde{h}_1 = 1/h_2$, $\tilde{h}_2 = 1$. We can then think of $\tilde{h}_2 = 1$ as the "new" h_1, and thus we have to interchange the subscripts 1 and 2, giving $\tilde{R} = Rh_2^3$. Thus, we must study the stability of the solution $\tilde{h} = 1$, with the parameters $\tilde{h}_2 = 1/h_2$, $\tilde{R} = Rh_2^3$, α. When we interchange the subscripts 1 and 2, we implicitly make a transformation $x \to -x$. Thus, the solution $\tilde{h} = 1$ with the parameters $\tilde{h}_2 = 1/h_2$, $\tilde{R} = Rh_2^3$, α is unstable if and only if the solution $h = 1$ with the parameters h_2, R, α is stable (we remind the reader that the system (3.27) is one dimensional, so there is only one stable or unstable direction at the fixed points). Finally, from (3.32), the condition of instability of the point $h = h_2$ is

$$R \tan\alpha < \frac{1}{h_2^3} f_1\left(\frac{1}{h_2}\right) = f_2(h_2), \tag{3.33}$$

where $f_1(h_2)$ is given by (3.32). Using (3.32), the condition (3.33) can be written explicitly as:

$$R \tan\alpha < \frac{15h_2}{-h_2^4 - 2h_2^3 + 3h_2^2 + 10h_2 + 5} = f_2(h_2). \tag{3.34}$$

Expression (3.34), of course, could also have been obtained directly from (3.27), but this derivation illuminates the symmetry.

We have already mentioned that we are interested in the solutions of the type illustrated in figure 3.1. Since $h = h_2 > 1$ and $h = 1$ are the fixed points and the height at the left end $x = -\infty$ must be larger than at the right end $x = +\infty$, the solution must start at $h = h_2$ and end at $h = 1$. Thus, $h = h_2$ must be unstable and $h = h_1$ stable. From the

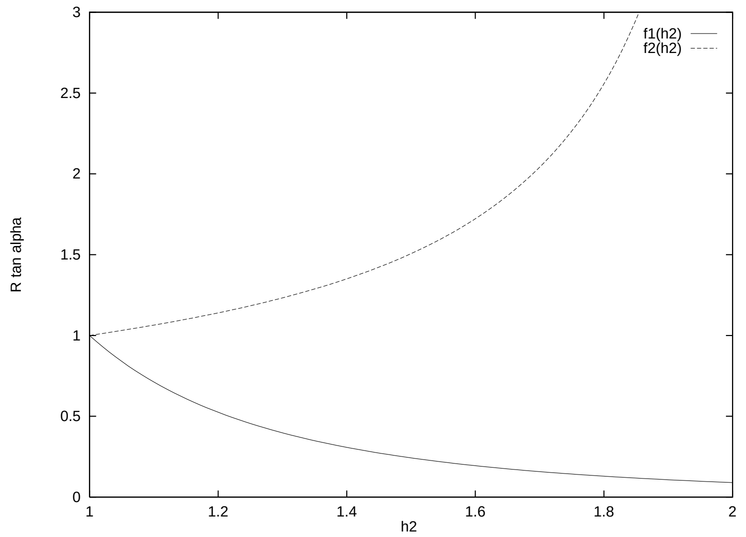

Figure 3.4: A plot of the functions $f_1(h_2)$ from (3.32) (solid line) and $f_2(h_2)$ from (3.34) (dashed line) versus h_2.

graph $f_1(h_2)$ and $f_2(h_2)$ shown in figure 3.4, one can deduce that for all $h_2 > 1$ we have $f_2(h_2) > f_1(h_2)$. Thus, the necessary condition for the existence of such solitary waves is just (3.32). However, the condition (3.32) by no means guarantees the existence of a solitary wave solution which smoothly joins the states $h = h_2$ and $h = 1$. Again, the problems can arise if at some $h = h_*$ the denominator on the right-hand side of (3.27) vanishes, and h' becomes infinite. The singular height has to satisfy equation (3.30). For the heteroclinic solution joining h_1 and h_2 to exist, we must either require that $h_* > h_2$ or $h_* < 1$. The condition $h_* > h_2$ can be rewritten as

$$R \tan\alpha > \frac{15h_2}{-h_2^4 - 2h_2^3 + 3h_2^2 + 10h_2 + 5} = f_2(h_2),$$

where $f_2(h_2)$ is the same as in (3.34). The condition $h_* < 1$ is now

$$R \tan\alpha < \frac{15}{5h_2^4 + 10h_2^3 + 3h_2^2 - 2h_2 - 1} = f_1(h_2),$$

which is the same as (3.32). Finally, we arrive to the conclusion that heteroclinic orbits in (3.27) exist only if (3.32) is satisfied.

Finally, in figure 3.5 we present a plot of a solution of (3.27) for the values of parameters $R = 1$, $\alpha = 5$deg and $h_2 = 1.5$. Condition (3.27) in this case gives $R < 2.774$.

Next, we introduce an extra shape parameter Λ, as we have done for the circular hydraulic jump in the previous chapter.

3.5.2 Introducing the shape parameter

The model (3.25) can be extended to allow a change in the velocity profile. The derivation of such a model is the same as the derivation of the system (2.42), except that we now have to deal with non-stationary flows.

As before, we approximate the velocity profile by a third-order polynomial $u(\xi, \eta) = v(a\eta + b\eta^2 + c\eta^3)$, identical to (2.36). Λ is the shape parameter, and we set $a = \Lambda + 13/2$,

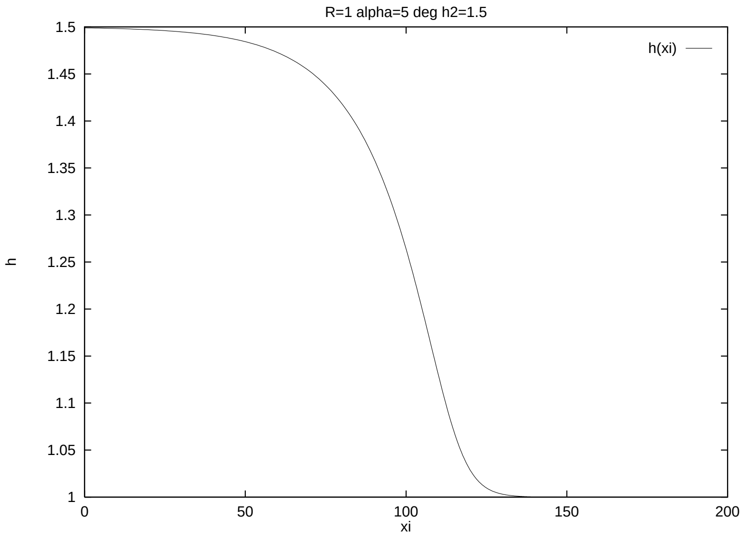

Figure 3.5: A solution of (3.27) for $R = 1, \alpha = 5$ deg and $h_2 = 1.5$ corresponding to $h_* < 1$.

$b = -5\Lambda/2 - 41/4$, $c = (4/3)\Lambda + 14/3$, as in (2.38). To obtain the evolution equations for $\Lambda(x,t)$ and $h(x,t)$, we use the flux conservation (3.22), the momentum equation (3.18.1) averaged with respect to y and the momentum equation (3.18.1) at $y = 0$. We get the following system:

$$\begin{aligned} & h_t + (hv)_x = 0 \\ & (hv)_t + (hv^2F_2)_x + \frac{3}{R}hh_x \cot\alpha = -\frac{1}{R}\frac{v}{h}\left(\Lambda + \frac{13}{2}\right) + \frac{3}{R}h \\ & h_x \cot\alpha = 1 - \frac{v}{3h^2}(5\Lambda + \frac{41}{2}). \end{aligned} \tag{3.35}$$

The system (3.25) is a simplified version of (3.35) where $\Lambda \equiv -7/2$ (the velocity profile is fixed to be parabolic) and the third equation of (3.35) is discarded.

Given the system (3.35), we shall look for solitary waves running down with a constant speed c. In (3.35), we substitute $h = h(\xi)$, $v = v(\xi)$ and $\Lambda = \Lambda(\xi)$, where $\xi = x - ct$. We get

$$\begin{aligned} & -ch_\xi + (hv)_\xi = 0 \\ & -c(hv)_\xi + (hv^2F_2)_\xi + \frac{3}{R}hh_\xi \cot\alpha = -\frac{1}{R}\frac{v}{h}\left(\Lambda + \tfrac{13}{2}\right) + \frac{3}{R}h \\ & h_\xi \cot\alpha = 1 - \frac{v}{3h^2}(5\Lambda + 41/2). \end{aligned} \tag{3.36}$$

Again, $h = 1$, $v = 1$ and $\Lambda = -7/2$ (parabolic profile) is a fixed point.

Solutions with vanishing height

If $c < 1$, there is only one fixed point $h = 1$. This fixed point is unstable when we integrate in the $-\xi$ direction, thus the trajectories starting close to $h = 1$ and $\Lambda = -7/2$ develop a singularity for finite ξ. We assume the following ansatz for the singularity

$$h = A(\xi - \xi_0), \tag{3.37}$$

where A is a constant. From (3.36.1) we see that the average velocity v diverges as

$$v \simeq \frac{1-c}{h} \simeq \frac{1-c}{A(\xi - \xi_0)} \tag{3.38}$$

and Λ must approach $-41/10$ as

$$\Lambda \simeq -41/10 + B(\xi - \xi_0)^3, \tag{3.39}$$

where B is a constant. Collecting the most singular terms in (3.36), we obtain the expression for the singular solution described by (3.37):

$$h \simeq \frac{12}{5RF_2^0} \frac{\xi - \xi_0}{1-c}, \tag{3.40}$$

where, again, $F_2^0 = F_2(\Lambda = -4.1) \simeq 1.2343$. The shape parameter Λ is given by

$$\Lambda = -\frac{41}{10} + (1 - A\cot\alpha)\frac{3}{5A^3(1-c)}(\xi - \xi_0)^3, \tag{3.41}$$

where $A = 12/(5RF_2^0)(1-c)$. The solutions with vanishing height seem to be realized for all values R, α and $c < 1$. These solutions can be easily obtained by starting close to the fixed point $h = 1$, $\Lambda = -7/2$ and integrating backward. However, there are two qualitatively different types of solutions. If Λ increases at the point $\xi = \xi_0$, the solution reaches the parabolic profile $\Lambda = -7/2$ very quickly, and the height profile is similar to the one illustrated in figure 3.3. The solution does not look like a shock, since it does not have a distinct shallow part. However, if Λ *decreases* at the singular point $h = 0, \Lambda = -41/10$, it takes longer for the solution to reach the value $\Lambda = -7/2$. The component Λ decreases at the singular point and the solution has a distinct 'shallow' part if

$$R\tan\alpha < \frac{2.4}{F_2^0}(1-c) \simeq 1.944(1-c). \tag{3.42}$$

Finally, in figure 3.6 we present a numerical solution for $c = 0$, $R = 5$ and $\alpha = 2$ deg, so $R\tan\alpha \simeq 0.157$ and (3.42) is satisfied. The solution indeed reminds us of a shock and could be presumably associated with the flow exiting a sluise gate, as illustrated in figure 3.2. We observe a fast 'shooting' flow before the shock and a slow flow after the shock. The slope of the solid line on figure 3.6 is given by (3.40). We see that the prediction (3.40) is quite accurate.

Heteroclinic solutions: $c > 1$

In the case $c > 1$, there are two solutions: $h \equiv h_1 = 1$ and $h \equiv h_2$ with $c = 1 + h_2 + h_2^2$. Recall that due to the symmetry $h_2 \to 1/h_2$, $R \to h_2^3 R$, we only need to study the region $h_2 > 1$, which corresponds to $c > 3$.

We shall look for a solitary wave propagating with a speed c and approaching the height $h_2 > 1$ at $x \to -\infty$ and $h_1 = 1$ at $x \to +\infty$. Such a solitary wave will be a heteroclinic orbit, connecting two fixed points on the phase plane (h, Λ): it starts from $(h_2, -7/2)$ and goes into $(1, -7/2)$. Thus, a necessary condition for the existence of such a

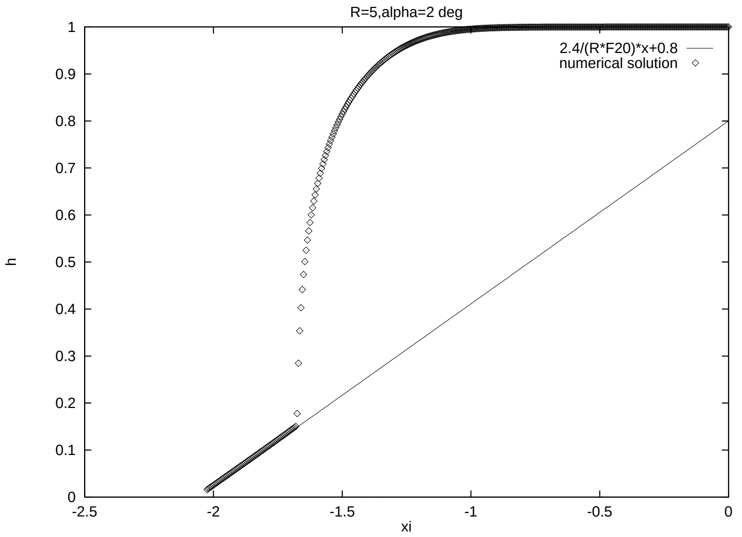

Figure 3.6: A numerical solution of (3.36) with $c = 0, R = 5, \alpha = 2$deg (diamonds). The asymptotic formula (3.40) is plotted as a solid line for comparison.

heteroclinic orbit is the presence of at least one unstable direction for the point $(h_2, -7/2)$ and at least one stable direction for the point $(1, -7/2)$.

Suppose we linearise the system (3.36) around a fixed point, which gives an equation for the disturbances δh and $\delta\Lambda$:

$$\begin{pmatrix} \delta h' \\ \delta\Lambda' \end{pmatrix} = J \begin{pmatrix} \delta h \\ \delta\Lambda \end{pmatrix} \tag{3.43}$$

where J is a 2×2 matrix – the Jacobi matrix of the system (3.36) evaluated at the fixed point where the primes denote derivatives with respect to ξ. The eigenvalues λ of the matrix J satisfy the characteristic equation:

$$\lambda^2 - (\mathrm{tr}J)\lambda + \det J = 0 \tag{3.44}$$

The eigenvalues λ_1 and λ_2 satisfy the relationships:

$$\begin{aligned} \lambda_1\lambda_2 &= \det J \\ \lambda_1 + \lambda_2 &= \mathrm{tr}J \end{aligned} \tag{3.45}$$

For the fixed point $h = 1$ and $\Lambda = -7/2$, the corresponding determinant and trace are

$$\begin{aligned} \det J_1(h_2, R, \alpha) &= 60(h_2^2 + h_2 - 2)/(R\tan\alpha) \\ \mathrm{tr}J_1(h_2, R, \alpha) &= -60/(R\tan\alpha) - 3 - 11h_2 + 14h_2^2 + 50h_2^3 + 25h_2^4. \end{aligned} \tag{3.46}$$

We are only interested in the case $h_2 > 1$, $\det J_1(h_2, R, \alpha) > 0$. If $\mathrm{tr}J_1(h_2, R, \alpha) < 0$, the point $h = 1, \Lambda = -7/2$ has two stable directions, and if $\mathrm{tr}J_1(h_2, R, \alpha) > 0$, there are two unstable directions. In fact, if the eigenvalues λ_1 and λ_2 are real, this follows from (3.45). If the eigenvalues λ_1 and λ_2 are complex, then $\mathrm{Re}\,\lambda_{1,2} = \mathrm{tr}J/2$. We only consider solutions going from the larger height at $x = -\infty$ to the smaller height at $x = +\infty$. Due to the symmetry, the study of the case $0 < h_2 < 1$ is completely analogous to the case $h_2 > 1$. Since $h_2 > h_1 = 1$, the solutions must exit from $h = h_2, \Lambda = -7/2$ and go into $h = 1, \Lambda = -7/2$. Thus, a solution can enter the fixed point $h = 1, \Lambda = -7/2$ if $\mathrm{tr}J_1(h_2, R, \alpha) < 0$, and in this case the fixed point is stable.

The stability of the second fixed point $h = h_2$, $\Lambda = -7/2$ can be calculated directly from (3.36). However, we shall employ symmetry considerations similar to the ones we used when analyzing the stability of the self-similar profile (3.27). We scale $h \to h/h_2$, in this case $\tilde{h}_2 = 1$, $\tilde{h}_1 = 1/h_2$. We interchange the symbols 1 and 2, which corresponds to taking $\tilde{x} = -x$ and transforming the Reynolds number to $\tilde{R} = Rh_2^3$. Also, the eigenvalues λ_i of the Jacobi matrix J have to be scaled under this transformation. In fact, the eigenvalues at the fixed points describe the growth of small linear perturbations away from the fixed point, for example,

$$\delta h \sim \sum_i C_i \exp\left(\lambda_i(h_2, R, \alpha)\xi\right), \tag{3.47}$$

where C_i are arbitrary constants. Thus, the eigenvalues have to be scaled as

$$\tilde{\lambda}(h_2, R, \alpha) = -\frac{1}{h_2}\lambda\left(\frac{1}{h_2}, Rh_2^3, \alpha\right). \tag{3.48}$$

Thus, the determinant and the trace of the Jacobi matrix at the fixed point $h = h_2$, $\Lambda = -7/2$ are given by

$$\begin{aligned} \det J_2(h_2, R, \alpha) &= \frac{1}{h_2^2} \det J_1\left(\tfrac{1}{h_2}, Rh_2^3, \alpha\right) \\ \mathrm{tr}J_2(h_2, R, \alpha) &= -\frac{1}{h_2}\mathrm{tr}J_1\left(\frac{1}{h_2}, Rh_2^3, \alpha\right). \end{aligned} \tag{3.49}$$

Inserting (3.46) into (3.49), we get

$$\begin{aligned} \det J_2(h_2, R, \alpha) &= 60(1 + h_2 - 2h_2^2)/(h_2^7 R \tan\alpha) \\ \mathrm{tr}J_2(h_2, R, \alpha) &= (60/(R\tan\alpha)h_2 + 3h_2^4 + 11h_2^3 - 14h_2^2 - 50h_2 - 25)/h_2^5. \end{aligned} \tag{3.50}$$

Since $\det J_2(h_2, R, \alpha) < 0$ for $h_2 > 1$, there is always one unstable direction at the fixed point $h = h_2$.

We see that a heteroclinic solution connecting different fixed points can exist if the fixed point $h = 1$, $\Lambda = -7/2$ is stable, which holds if

$$R\tan\alpha < f_s(h_2) = \frac{60}{-3 - 11h_2 + 14h_2^2 + 50h_2^3 + 25h_2^4}. \tag{3.51}$$

We find numerically that the condition (3.51) also seems to be sufficient. For any R and α we have tried in the range (3.51) a heteroclinic solution could be found.

We shall also note that the solution starts oscillating when approaching the fixed point $h = 1$, $\Lambda = -7/2$ if the eigenvalues $\lambda_{1,2}$ are complex, i.e. if $\mathrm{tr}J_1^2 - 4\det J_1 < 0$. This

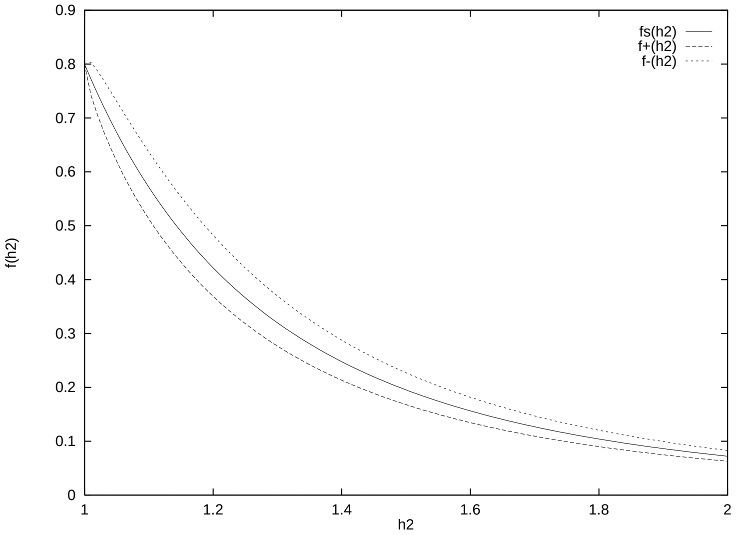

Figure 3.7: Functions $f_s(h_2)$ (given by (3.51)) and $f_\pm(h_2)$ (given by (3.52)).

corresponds to the values of $R\tan\alpha$ lying between $f_+(h_2)$ and $f_-(h_2)$, where the functions $f_\pm(h_2)$ are given by

$$f_\pm(h_2) = \frac{60}{-7 - 9h_2 + 16h_2^2 + 50h_2^3 + 25h_2^4 \pm 2\sqrt{5D}}, \tag{3.52}$$

where

$$D = 2 + 3h_2 - 9h_2^2 - 19h_2^3 + 3h_2^4 + 15h_2^5 + 5h_2^6.$$

We present a plot of functions $f_s(h_2)$ given by (3.51) and $f_\pm(h_2)$ from (3.52) in figure 3.7. One can see that $f_+(h_2) < f_s(h_2) < f_(h_2)$. Thus, the solution will have an oscillatory character when $R\tan\alpha$ is sufficiently close to the critical value given by (3.51).

Several solutions of the system (3.36) for different values of R are presented in figure 3.8 ($h_2 = 1.5 > 1$, h as a function of ξ) and figure 3.9 (the same values of the parameter h_2, Λ as a function of ξ). The value of the inclination angle α was 2 degrees for all solutions. Condition (3.51) yields $R < 5.591$ for $h_2 = 1.5, \alpha = 2\,\mathrm{deg}$. The solution becomes oscillatory due to (3.52) if $R > f_+(h_2)/\tan\alpha \simeq 4.809$. The oscillations become very pronounced when R approaches the critical value given by (3.51).

3.6 Linear stability of stationary states

The integral method allows us not only to predict the stationary solutions, but also to compute the evolution of small disturbances for the fixed points $h = const$. In what follows, we shall also take surface tension effects into account, since they are important for the evolution of short waves. In principle, one could also try to find the stationary solutions and solitary waves taking the surface tension effects into account (see, for example, [4]). However, the inclusion of surface tension increases the order of the system (3.35) and makes the analysis difficult.

Two questions will be of interest to us. First, are the solutions derived above true shocks? In other words, is the flow supercritical in front of the shock and subcritical after

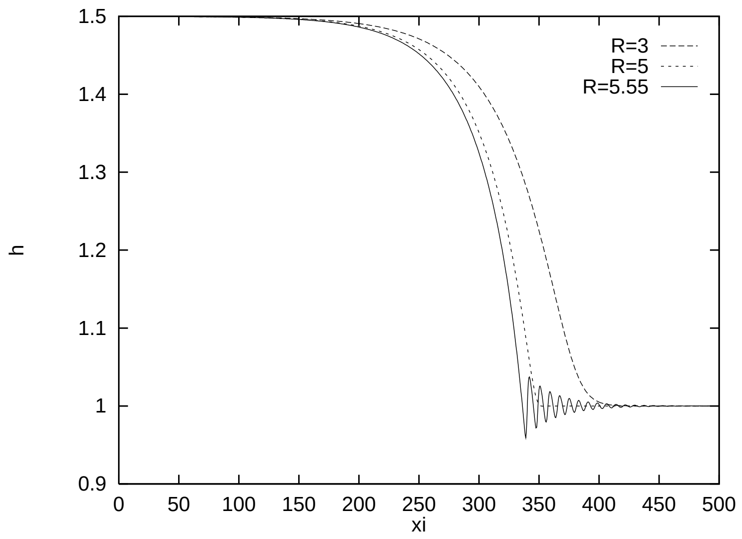

Figure 3.8: Height as a function of ξ for different values of R. Here $h_2 = 1.5$, $\alpha = 2$deg.

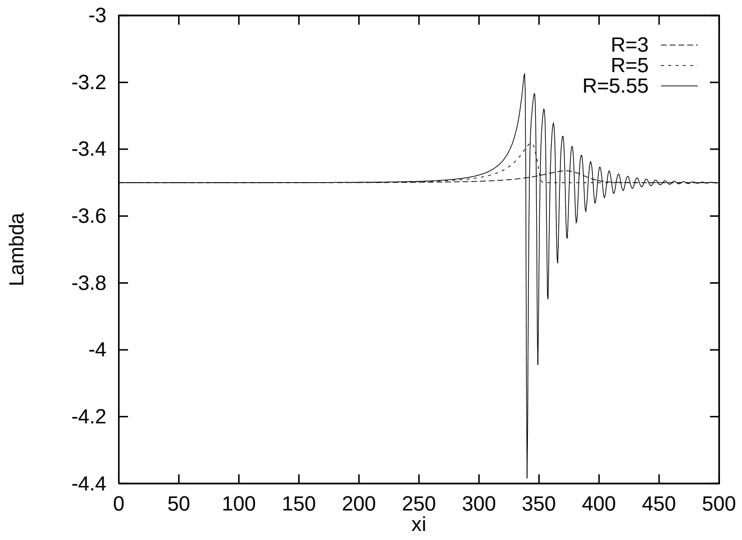

Figure 3.9: Shape parameter Λ as a function of ξ for different values of R. Here $h_2 = 1.5$, $\alpha = 2$deg, as before.

the shock? We remind the reader that a shock separates a supercritical region from a subcritical one; the flow is subcritical if the disturbances propagate both upstream and downstream relative to the shock, and supercritical if the disturbances only propagate upstream (towards the shock). Second, are these solutions stable? The answer to these questions is provided by the integral model. We recall that when $c < 1$, the state $h = 1$ is situated after the shock. Therefore, for $c < 1$, the state $h = 1$ must be subcritical and stable. On the contrary, for the moving shocks with $h_2 > 1$ the state $h = 1$ is situated before the shock, so this state must be supercritical. On the contrary, the state $h = h_2$ is situated after the shock and therefore must be subcritical.

First, we shall perform linear stability analysis for the self-similar model (3.25), and then for the more sophisticated (3.35). We shall see that the model (3.35), in which the velocity profile is allowed to change, predicts a transition to supercriticality at intermediate wavelengths. This results cannot be obtained from (3.25), where the velocity profile is fixed to be parabolic. But before we start our analysis, we shall discuss how to include surface tension effects in the systems (3.25) and (3.35).

3.6.1 Inclusion of surface tension effects

The surface tension introduces the difference between the external pressure and the pressure inside the fluid. If the surface tension coefficient is σ, the pressure inside the fluid has to *decrease* by $\sigma h''$, provided that the inclination of the free surface h' is assumed small. The extra pressure gradient is thus $-\sigma h'''$. If the height downstream h_1 given by (3.10) is used as the length scale, the system (3.18) transforms to

$$\begin{aligned} & u_t + uu_x + wu_y = -\frac{3}{R}h_x \cot\alpha + \frac{1}{R}u_{yy} + \frac{3}{R} + Wh_{xxx} \\ & u_\xi + w_y = 0, \end{aligned} \tag{3.53}$$

where

$$W = \frac{\sigma}{\rho h_1 v_1^2} = \frac{9\sigma}{\rho g h_1^2 \sin^2\alpha} \tag{3.54}$$

is the Weber number. We can now repeat the derivation of (3.25) and (3.35) starting with these modified boundary layer equations (3.53). The system (3.25), obtained by the self-similar ansatz, transforms to:

$$\begin{aligned} & h_t + (vh)_x = 0 \\ & (hv)_t + (hv^2F_2)_x + \frac{3}{R}hh_x\cot\alpha = -\frac{3}{R}\frac{v}{h} + \frac{3}{R}h + Whh_{xxx}, \end{aligned} \tag{3.55}$$

which is called the Shkadov model for the inclined plane waves.

The more general system (3.35), containing the shape parameter Λ, becomes:

$$\begin{aligned} & h_t + (hv)_x = 0 \\ & (hv)_t + (hv^2F_2)_x + \frac{3}{R}hh_x\cot\alpha = -\frac{1}{R}\frac{v}{h}\left(\Lambda + \frac{13}{2}\right) + \frac{3}{R}h + Whh_{xxx} \\ & h_x\cot\alpha = 1 - \frac{v}{3h^2}(5\Lambda + 41/2) + \frac{WR}{3}h_{xxx}. \end{aligned} \tag{3.56}$$

Ideally, one would like to linearise (3.55) and (3.56) around the stationary solutions (or solitary waves) found before and find the dispersion relation for the disturbances. This is, however, difficult to realize analytically, since the stationary solutions and the solitary waves are known only numerically. We shall therefore assume that we are sufficiently far from the shocks and the solution has converged to the state $h = const$ and $\Lambda = const$.

We shall start with the linear stability analysis of the state $h = 1, \Lambda = -7/2$. We have assumed without loss of generality that this state always describes the flow downstream. For stationary states $c = 0$ (flow exiting a sluice, see figure 3.2), this state describes a flow *after the shock*, and we want it to be subcritical and stable.

3.6.2 Linear stability of the stationary states

We perform the linear stability analysis of the models (3.55) and (3.56) around the fixed points $h = 1$, $v = 1$. As usual, we start with the simpler version (3.55).

3.6.3 Linear stability analysis for Shkadov model

To find the linear stability, we linearise (3.55) around the fixed point $h = 1, v = 1$: $v = 1 + v_1(x,t)$, $h = 1 + h_1(x,t)$. Then, (3.25) becomes:

$$\begin{aligned} &h_{1,t} + h_{1,x} + v_{1,x} = 0 \\ &v_{1,t} + h_{1,t} + 2F_2 v_{1,x} + F_2 h_{1,x} + \frac{3}{R}\cot\alpha h_{1,x} = -\frac{3}{R}v_1 + \frac{6}{R}h_1 + W h_{1,xxx}. \end{aligned} \tag{3.57}$$

Recall that in this model $F_2 = 6/5 = const$. We shall now assume that the disturbances are linear waves

$$\begin{aligned} v_1 &= V_1 e^{i(kx-\omega t)} \\ h_1 &= H_1 e^{i(kx-\omega t)}, \end{aligned} \tag{3.58}$$

where V_1 and H_1 are constants, ω is the complex frequency and k is the wavenumber. $\operatorname{Im}\omega$ is the stability coefficient with $\operatorname{Im}\omega > 0$ corresponding to stability and $\operatorname{Im}\omega < 0$ to the instability. The real part of ω describes the velocity of the waves, or more precisely, the waves propagate with group velocity

$$v(k) = \frac{d}{dk}\operatorname{Re}\omega. \tag{3.59}$$

Substitution of the mode (3.58) into (3.57) gives two linear homogeneous equations in H_1 and V_1:

$$\begin{aligned} &(-i\omega + ik)H_1 + ikV_1 = 0 \\ &(-i\omega + F_2 ik + \frac{3}{R}\cot\alpha ik - \frac{6}{R} + iWk^3)H_1 + (-i\omega + 2F_2 ik + \frac{3}{R})V_1 = 0. \end{aligned} \tag{3.60}$$

A non-trivial solution of the system (3.60) is possible if the determinant of the corresponding matrix is zero, which affords the relationship between ω and k:

$$\omega^2 + \omega\left(-\frac{12}{5}k + i\frac{3}{R}\right) + \left(\frac{6}{5}k^2 - \frac{3}{R}k^2\cot\alpha - \frac{9}{R}ik - Wk^4\right) = 0, \tag{3.61}$$

which can be solved to provide the explicit dispersion relation $\omega(k)$:

$$\omega = \frac{1}{2}\left(-\frac{12}{5}k + i\frac{3}{R} \pm \sqrt{\frac{24}{25}k^2 + \frac{12}{R}k^2\cot\alpha + \frac{252}{5R}ik - \frac{9}{R^2} + 4Wk^4}\right). \tag{3.62}$$

Long wave limit

In the long wave limit $k \to 0$, (3.62) becomes

$$\begin{aligned} \omega_+ &= 3k + ik^2(R - \cot\alpha) - \frac{6}{5}k^3R(R - \cot\alpha) + O(k^4) \\ \omega_- &= -\tfrac{3}{5}k - \tfrac{3i}{R} + ik^2(\cot\alpha - R) + \frac{6}{5}k^3R(R - \cot\alpha) + O(k^4) \end{aligned} \tag{3.63}$$

For very small k, the flow is subcritical, since the group velocity $d\omega_+/dk = 3 > 0$ and $d\omega_+/dk = -3/5 < 0$. The branch ω_- is always stable, and ω_+ is stable if

$$R\tan\alpha < 1. \tag{3.64}$$

Intermediate values of k

For intermdiate values of k, the behavior is governed by the higher order terms in (3.63). Since the leading terms $O(k^3)$ for ω_+ and ω_- in (3.63) have opposite signs, the flow will be subcritical.

Short wave limit

For large k (the short wave limit) the dispersion relation (3.62) becomes:

$$\begin{aligned} \operatorname{Re}\omega_\pm &= \pm\sqrt{W}k^2 + O(k) \\ \operatorname{Im}\omega_\pm &= -\frac{3}{2R} + O(1/k). \end{aligned} \tag{3.65}$$

Thus, (3.55) is stable in the short wave limit if $W > 0$.

If $W = 0$ (the surface tension is absent), the dispersion relation (3.62) gives

$$\omega_\pm = c_\pm k - \frac{3i}{2R}\frac{c_\pm - 3}{c_\pm - 6/5} + O(k^{-1}). \tag{3.66}$$

Here $c_\pm$ is the velocity of the corresponding wave given by

$$c_\pm = \frac{6}{5} \pm \sqrt{\frac{6}{25} + \frac{3}{R\tan\alpha}}. \tag{3.67}$$

We see that $c_+ > 6/5$, thus the condition for the stability of the branch ω_+ is $c_+ < 3$, which is equivalent to

$$R\tan\alpha < 1. \tag{3.68}$$

The wave ω_- propagates upstream (and the flow is subcritical) if $c_- < 0$ in (3.67), which corresponds to

$$R\tan\alpha < \frac{5}{2}. \tag{3.69}$$

One can also deduce from (3.65) that the branch ω_- is always stable, since $c_- < 6/5$ from (3.67).

The linear stability analysis of the Shkadov model (3.55) is complete. We shall now perform the corresponding analysis of the equations (3.56).

3.6.4 Stability analysis of the averaged equations

We perform the linear stability analysis of (3.56) around the fixed point $v = 1$, $h = 1$, $\Lambda = -7/2$. Again, we put $v = 1 + v_1$, $h = 1 + h_1$, $\Lambda = -7/2 + \Lambda_1$ and assume the travelling wave ansatz for the disturbances $h_1, \Lambda_1, v_1 \sim e^{i(\omega t - kx)}$. We arrive at the following dispersion relation:

$$\begin{vmatrix} -i\omega + ik & ik & 0 \\ -i\omega + \left(\frac{6}{5} + 3ik\frac{\cot\alpha}{R}\right) - \frac{6}{R} + ik^3 W & -i\omega + \frac{12}{5}ik + \frac{3}{R} & -i\frac{k}{15} + \frac{1}{R} \\ i\cot\alpha k + i\frac{WR}{3}k^3 - 2 & 1 & \frac{5}{3} \end{vmatrix} = 0 \tag{3.70}$$

which can be transformed to

$$\begin{aligned} &a\omega^2 + b(k)\omega + c(k) = 0, \text{ where} \\ &a = -5/3 \\ &b(k) = \frac{61}{15}k - \frac{4i}{R} \\ &c(k) = \frac{12ik}{R} + \left(\frac{4}{R}\cot\alpha - \frac{11}{5}\right)k^2 + \frac{i}{15}\cot\alpha k^3 + \frac{4}{3}Wk^4 + \frac{i}{45}Wk^5. \end{aligned} \tag{3.71}$$

The explicit disperison relationship $\omega = \omega(k)$ can now be deduced from (3.71). We have

$$\omega_\pm = \frac{1}{2a}\left(-b(k) \pm \sqrt{b(k)^2 - 4ac(k)}\right) \tag{3.72}$$

Long wave limit

First, we analyze (3.72) in the long wavelength limit $k \to 0$. The two dispersion branches $\omega_\pm$ behave as

$$\begin{aligned} \omega_+(k) &= 3k + \frac{5}{4}ik^2(R - \frac{4}{5}\cot\alpha) + \frac{89}{48}Rk^3(\frac{72}{89}\cot\alpha - R) + O(k^4) \\ \omega_-(k) &= -\frac{14}{25}k - \frac{12}{5R}i + \frac{5}{4}ik^2(-R + \cot\alpha) + \frac{89}{48}Rk^3(R - \frac{72}{89}\cot\alpha) + O(k^4). \end{aligned} \tag{3.73}$$

Thus, in the long wave limit the flow is subcritical since ω_- is propagating backward with velocity $-14/25$. The ω_+ branch is stable if

$$R\tan\alpha < \frac{4}{5}. \tag{3.74}$$

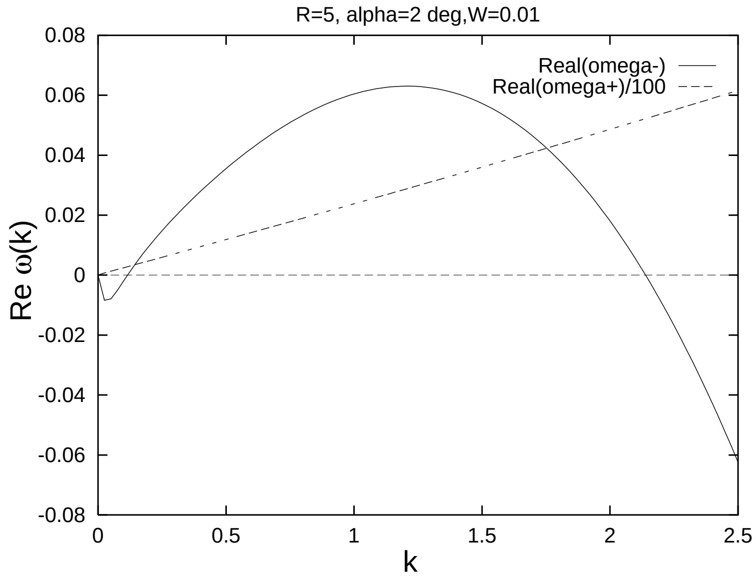

Figure 3.10: Real part of $\omega_\pm$ versus k.

Intermediate wave limit: supercriticality

As we remember, the Shkadov model was subcritical in the intermediate k regime. The model (3.35), on the other hand, exibits a transition from the sub- to supercritical regime for intermediate k. To illustrate this, we plot the real part of $\omega_\pm(k)$ from (3.72) on figure 3.10. One can see that the subcritical behaviour emerging in the limit $k \to 0$, is in fact realized for a very tiny region in k. The group velocity given by $d\omega_+(k)/dk$ is always positive, and the group velocity $d\omega_-(k)/dk$ is positive if k is large, but not too large. The behaviour of the branch ω_- in (3.73) for the intermediate values of k is governed by the $O(k^3)$ terms. From the second equation of (3.73) we obtain the condition for the slope of $\omega_-(k)$ to be negative for intermediate k (which is the condition for subcriticality of the flow):

$$R \tan\alpha < \frac{72}{89}. \tag{3.75}$$

Short wave limit: ultraviolet catastrophe

For large k, the frequency ω behaves as

$$\omega_\pm \sim \pm k^{5/2}\sqrt{i\frac{W}{75}}, \tag{3.76}$$

if $W > 0$ and

$$\omega_\pm \sim \pm k^{3/2}\sqrt{i\frac{\cot\alpha}{25}} \tag{3.77}$$

if $W = 0$. In both cases the frequency of one of the branches has an imaginary part, growing to $+\infty$ very quickly as $k \to \infty$. This instability is unphysical and caused by the fact that the evolution of very short waves is approximated badly by the boundary layer approximation. In fact, in the boundary layer equations (3.18) the high derivatives of the velocity with respect to x are neglected. It is thus surprising that the Shkadov model (3.55) provides a reasonable behaviour for large k.

A physical way to cure the instability for large k is to introduce smoothing (averaging) over the short distances in x. We rewrite the third equation of (3.56) as

$$\int_{-\infty}^{+\infty} g(x-s)\left(h_x \cot\alpha - \frac{RW}{3}h_{xxx}\right)(s)\mathrm{d}s = 1 - \frac{v}{3h^2}(5\Lambda + 41/2). \tag{3.78}$$

Here $g(x)$ is the smoothing function

$$g(x) = g_0 e^{-\pi g_0^2 x^2}. \tag{3.79}$$

In the limit $g_0 \to \infty$ the function $g(x)$ becomes the delta-function and (3.78) transforms exactly into the third equation of (3.56).

We shall thus consider the linear stability of the stationary state $h = 1$, $v = 1$ and $\Lambda = -7/2$ of the system

$$\begin{aligned}
&h_t + (hv)_x = 0\\
&(hv)_t + (hv^2F_2)_x + \frac{3}{R}hh_x\cot\alpha = -\tfrac{1}{R}\tfrac{v}{h}\left(\Lambda + \tfrac{13}{2}\right) + \frac{3}{R}h + \tfrac{R}{3}Wh_{xxx}\\
&\textstyle\int_{-\infty}^{+\infty} g(x-s)\left(h_x\cot\alpha - \frac{RW}{3}h_{xxx}\right)(s)\mathrm{d}s = 1 - \dfrac{v}{3h^2}(5\Lambda + 41/2).
\end{aligned} \tag{3.80}$$

We linearize the solution around the stationary state $h = 1 + h_1$, $v = 1 + v_1$ and $\Lambda = -7/2 + \Lambda_1$. Assuming the travelling wave ansatz for the disturbances and taking into account that

$$\int_{-\infty}^{+\infty} g_0 e^{-\pi g_0^2 x^2} e^{iks}\mathrm{d}s = e^{-\dfrac{k^2}{4\pi g_0^2}}, \tag{3.81}$$

we get the following dispersion relation:

$$\begin{vmatrix}
-i\omega + ik & ik & 0\\
-i\omega + \left(\frac{6}{5} + 3ik\frac{\cot\alpha}{R}\right) - \frac{6}{R} + ik^3W & -i\omega + \frac{12}{5}ik + \frac{3}{R} & -i\frac{k}{15} + \frac{1}{R}\\
(i\cot\alpha k + i\frac{WR}{3}k^3)e^{-k^2/(4\pi g_0^2)} - 2 & 1 & \frac{5}{3}
\end{vmatrix} = 0. \tag{3.82}$$

One can notice an important difference between (3.70) and (3.82): in the third row of the matrix (3.82) the high powers of k are multiplied by the cutoff function (3.81). The cutoff size in k is equal to

$$k_0 = 2g_0\sqrt{\pi}. \tag{3.83}$$

For k much larger than the cutoff k_0, the dispersion relation (3.82) simplifies to

$$-\frac{5}{3}\omega^2 + \left(\frac{61}{2}k - \frac{4i}{R}\right) + \frac{5\cot\alpha}{R}k^2 - \frac{31}{15}k^2 + \frac{14ik}{R} + \frac{5}{3}Wk^4 = 0. \tag{3.84}$$

If $W > 0$, the solution of (3.84) behaves asymptotically as

$$\begin{aligned} \mathrm{Re}\,\omega_\pm &= \pm\sqrt{W}k^2 + O(k) \\ \mathrm{Im}\,\omega_\pm &= -\frac{6}{5R} + O(1/k). \end{aligned} \tag{3.85}$$

Thus, both dispersion branches $\omega_\pm$ are now stable in the limit $k \to \infty$.

If $W = 0$, the asymptotics $\omega_\pm$ are

$$\omega_\pm \sim c_\pm k - \frac{6i}{5R}\frac{c_\pm - 7/2}{c_\pm - 61/50}, \tag{3.86}$$

where the velocity of the linear waves $c_\pm$ is given by

$$c_\pm = \frac{61}{50} \pm \sqrt{\left(\frac{61}{50}\right)^2 + 4\left(\frac{3}{R\tan\alpha} - \frac{31}{25}\right)} \tag{3.87}$$

Since $c_+ > 61/50$, the condition for the stability of ω_+ is $c_+ > 7/2$, or

$$R\tan\alpha < \frac{20}{33}. \tag{3.88}$$

Since $c_- < 6/5$, the branch ω_- is always stable. The flow is supercritical, if $c_- < 0$, which is equivalent to

$$R\tan\alpha < \frac{75}{31}. \tag{3.89}$$

3.6.5 Stability analysis of moving solitary waves

In the case of a moving solitary wave, super- and sub-criticality have to be defined in a system of coordinates, moving together with the wave at velocity c. Thus, we call the flow supercritical if the group velocity of the waves is less than c, and subcritical, if one of the group velocities is larger than c and one is smaller than c. We shall be interested in the case when $h_2 > 1$, so $c = 1 + h_2 + h_2^2 > 3$.

Technically, we have to perform the linear stability analysis around the solution $h \equiv h_2$, $\Lambda \equiv -7/2$. We can, however, rescale the height by h_2. In this case, the wavenumber k has to be multiplied by h_2, the Reynolds number has to be multiplied by h_2^3 and the Weber number by h_2. The frequency ω also has to be rescaled. The velocity has to be scaled by $q_2/h_2 = h_2^2$, thus time has to be scaled as velocity/height=h_2. Let us call $\omega_{h_2}(k, R, W, \alpha)$ the dispersion relation for the evolution of linear waves around the state $h = h_2$ with Reynolds number R and Weber number W, and call $\omega(k, R, W, \alpha)$ the corresponding dispersion relation for the state $h = 1$. Then, ω_{h_2} and ω are connected by the following scaling formula:

$$\omega_{h_2}(k, R, W, \alpha) = h_2\omega(kh_2, Rh_2^3, Wh_2^2, \alpha). \tag{3.90}$$

For the reader who is not convinced by the scaling argument, we present the analogues of the equations for the dispersion relations (3.61) and (3.71), where the linearization is performed around the height $h = h_2$. For the Shkadov model (3.55), the dispersion relation becomes:

$$h_2\omega^2 + \omega\left(-\frac{12}{5}h_2^3k + \frac{3i}{Rh_2}\right) + \left(\frac{6}{5}h_2^5k^2 - \frac{3}{R}h_2^2\cot\alpha k^2 - \frac{9}{R}h_2 ik - Wh_2^2k^4\right) = 0. \tag{3.91}$$

For the model (3.35), the dispersion relation for the linear waves is:

$$
\begin{aligned}
& a\omega^2 + b(k)\omega + c(k) = 0, \ \text{where} \\
& a = -5/3h_2 \\
& b(k) = \tfrac{61}{15}kh_2^3 - \frac{4i}{Rh_2} \\
& c(k) = \tfrac{12ik}{R}h_2 + \left(\tfrac{4}{R}h_2^2\cot\alpha - \tfrac{11}{5}h_2^5\right)k^2 + \tfrac{i}{15}\cot\alpha h_2^6 k^3 + \\
& \tfrac{4}{3}h_2^4 W k^4 + \tfrac{i}{45}h_2^6 W k^5.
\end{aligned}
\tag{3.92}
$$

One can see that (3.90) is indeed satisfied. Now, the remaining stability analysis of the flow before and after the shock (solitary wave) is straightforward.

3.6.6 Super- and subcriticality in the Shkadov model

We investigate super- and sub- criticality in the long wave limit $k \to 0$. For the state $h = 1$, linear waves propagate forward with the speed $d\omega_+/dk = 3$ and backward with speed $d\omega_-/dk = -3/5$ according to (3.63). Since we assume $h_2 > 1$, the shock velocity is $c = 1 + h_2 + h_2^2 > 3$ and the flow in front of the solitary wave is supercritical. In fact, in the system of coordinates moving with the shock, $d\omega_+/dk - c < 0$ and $d\omega_-/dk - c < 0$.

On the other hand, the velocity of wave after the solitary waves in the laboratory system of coordinates is $3h_2^2$ and $-(3/5)h_2^2$ due to the scaling relationship (3.90). It is easy to show that $3h_2^2 > c = 1 + h_2 + h_2^2$ for $h_2 > 1$, thus the flow after the solitary wave is subcritical.

The condition for stability of the state $h = h_2$ is provided by (3.64) and (3.90):

$$R\tan\alpha < \frac{1}{h_2^3}. \tag{3.93}$$

Now, we repeat this analysis for the averaged model (3.56).

3.6.7 Super- and subcriticality in the averaged model

Again, we shall only consider the long wave limit $k \to 0$. Linear disturbances propagate to the right with speed $d\omega_+/dk = 3$ and backward with the speed $d\omega_-/dk = -14/25$ due to (3.73). Analogously to the analysis of the Shkadov model, we conclude that the flow before the solitary wave is always supercritical, whereas behind the solitary wave the flow is always subcritical. Thus, a solitary wave in the model (3.56) is a classical shock. The condition for the stability of the state $h = h_2$, $\Lambda = -7/2$ in the long wave limit can be deduced from (3.74) and (3.90):

$$R\tan\alpha < \frac{4}{5h_2^3}. \tag{3.94}$$

We also note that in (3.93) and (3.94) we have used the Reynolds number R defined *downstream*. If we define R using the flux upstream q_2 as $R = q_2/\nu$, then (3.93) and (3.94) become $R\tan\alpha < 1$ and $R\tan\alpha < 4/5$, respectively.

3.7 Conclusion

After all the analysis performed in this chapter, we can conclude that we have described shocks in flows of water running down inclined planes. The main conclusion is that if the slope of the inclined plane is small enough, or if the water downstream is moving very slowly, so $R \tan \alpha$ is sufficiently small, then shocks can be formed. It is very interesting that the conditions for the existence of solitary waves and their stability are

$$R \tan \alpha < \text{some number of order } 1.$$

This also applies to the stationary solutions: a flow exiting sluice gates has a shock structure (a distinct fast shallow part, followed by a deep, slow moving part) and the flow in the slow part is sub-critical if

$$R \tan \alpha < \text{some number of order } 1.$$

The precise critical values of the numbers depend on the model. However, we believe that the major conclusion of this chapter is that some major changes of the flow structure occur when $R \tan \alpha \simeq 1$. We have been successful in describing the flow for values of $R \tan \alpha$ up to of order unity. Presumably, the description of the flow for very large $R \tan \alpha$ will require the inclusion of effects, neglected in our model, for example, turbulent viscosity. We shall summarise the results of this chapter in Table 3.1. We remind the reader that the state $h = 1$ is situated after the shock for $0 \leq c \leq 1$ and before the shock for $c > 3$ ($h_2 > 1$). The state $h = h_2$ is always after the shock.

Finally, we mention that in this chapter we have not emphasized the role played by the boundary layer separation. The separation bubble does not play an essential role for the inclined plane waves, as it does for the circular hydraulic jump. We shall just mention that it is possible for the averaged equations (3.35) to describe flows containing a separation of boundary layers. In figure 3.9, Λ reaches below the value $\Lambda = -7/2$ (which corresponds to the separation) in the oscillating part of the solution for $R = 5.55$. We thus believe that integral methods developed in this chapter can be used to study many classical problems of free-surface flows, where the separation of boundary layer plays a major role.

Table 3.1: Existence, stability and supercriticality for different models

Property	Regime	State	Model	Values of $R\tan\alpha$
Heteroclinic			(3.27)	$R\tan\alpha < 15/(5h_2^4 + 10h_2^3 + 3h_2^2 - 2h_2 - 1)$
Stability	low k	$h = 1$	(3.55)	$R\tan\alpha < 1$
Subcriticality	low k	$h = 1$	(3.55)	Always
Stability	high k	$h = 1$	(3.55) W=0	$R\tan\alpha < 1$
Subcriticality	high k	$h = 1$	(3.55) W=0	$R\tan\alpha < 5/2$
Stability	low k	$h = h_2$	(3.55)	$R\tan\alpha < 1/h_2^3$
Supercriticality	low k	$h = h_2$	(3.55)	Always
Shocks		$h = 1$	(3.56)	$R\tan\alpha < 1.944(1 - c)$
Stability	low k	$h = 1$	(3.56)	$R\tan\alpha < 4/5$
Subcriticality	low k	$h = 1$	(3.56)	Always
Subcriticality	intermediate k	$h = 1$	(3.56)	$R\tan\alpha < 72/89$
Stability	high k	$h = 1$	(3.80)	$R\tan\alpha < 20/33$
Subcriticality	high k	$h = 1$	(3.80)	$R\tan\alpha < 75/31$
Heteroclinic			(3.35)	$R\tan\alpha < 60/(25h_2^4 + 50h_2^3 + 14h_2^2 - 11h_2 - 3)$
Stability	low k	$h = h_2$	(3.56)	$R\tan\alpha < 4/(5h_2^3)$
Supercriticality	low k	$h = h_2$	(3.56)	Always

Bibliography

[1] Kapitsa, P. L. & Kapitsa, S. P., (1965) in *Collected works by P. L. Kapitsa*, Pergamon.

[2] Nakaya C. (1975) *Phys. Fluids*, **18**, 1407.

[3] Chang H.-C.,(1993) *J. Fluid Mech.*, **250**, 433.
Chang, H.-C. (1993) *Ann. Rev. Fluid Mech*, **26**, 103.

[4] Pumir A., Manneville P. & Pomeaux Y. (1983) *J. Fluid Mech.* **135**, 27.

[5] Whitham, G.B. (1974) *Linear and Nonlinear Waves* , Wiley-Interscience.